Journal of Materials Chemistry C

Accepted Manuscript

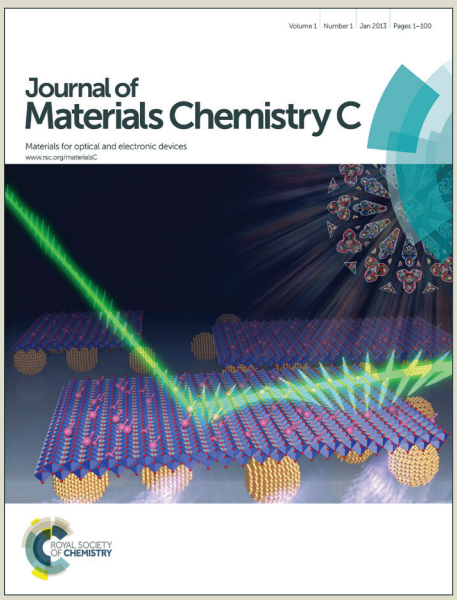

ROYAL SOCIETY OF CHEMISTRY

www.rsc.org/materialsC

Journal Name

ARTICLE

Reversible colorless-cyan photochromism in Eu^{2+}-doped $Sr_3YNa(PO_4)_3F$ powders

Received 00th January 20xx,
Accepted 00th January 20xx

DOI: 10.1039/x0xx00000x

www.rsc.org/

Yahong Jin, Yihua Hu,* Yinrong Fu, Li Chen, Guifang Ju and Zhongfei Mu

Photochromic materials have attracted increasing interests as optical switchers and erasable optical memory media. Here, we report on a novel reversible colorless-cyan photochromic powder material $Sr_3YNa(PO_4)_3F:Eu^{2+}$. The photochromic properties including coloring and bleaching are characterized by reflectance spectra after the powder is irradiated by different wavelength light for different irradiation times or thermal treatment. The results turn out that it can be colored by short wavelength light (200-320 nm) and bleached by longer wavelength light (320-800 nm) or thermal treatment at 240 ° C. The optimal doping concentration of Eu^{2+} is determined to be about 0.5 mol%. It shows high fatigue resistance in photochromism performance. Electrons in 4f ground levels excited by short wavelength irradiation to higher 5d states of Eu^{2+} and then captured by traps are responsible for the coloring process. Correspondingly, the releasing of trapped electrons from two kinds of traps with different depths causes the initially fast and later slow bleaching processes. The critical role of charge carrier motions between two different traps is discussed. The colorless-cyan photochromism can be explained semi-quantitatively on the basis of obtained results. A tentative model was proposed to illustrate the PC mechanism.

1. Introduction

Photochromism (PC), as a reversible transformation phenomenon, refers to the conversion of a chemical species between two states or two forms having distinguishably different absorption spectra, induced in at least one direction by incident electromagnetic radiation [1-7]. Such a light induced modification of some physical properties including electron conductivity, magnetic properties, refractive index, absorption spectra and geometrical structure may be tuned in photochromic materials [8, 9]. Photochromic materials have attracted considerable interests due to the reversible color changes that they can be colored when irradiated by light with a certain wavelength and later bleached upon thermal treatment or exposure to light with another different wavelength. This makes them find promising applications in various fields extending from rewritable copy papers, refractive-index modulators for optical fibers and communications, erasable optical memory media and sensors, photo-electronic devices to photo-optical switchers [10-16], etc.

In the past, numerous efforts have been devoted into the research of organic compounds including spiropyrans/oxazines, diarylethenes, fulgides, and azobenzenes for developing PC materials. However, some inherent drawbacks such as low thermal and chemical stability and environmentally harmful synthesis processes largely limit their commercial applications. In contrast, inorganic PC materials possess some superior properties over the organic counterparts due to their easily controllable macroscopic shape molding, high thermal and chemical stability and mechanical strength.

Motivated by this, some efforts have been made previously, and they have led to the discovery of some excellent PC materials based on inorganic compounds. Over the last 50 years, the study of inorganic photochromic materials has mainly focused on transition metal oxide thin films such as WO_3, MoO_3, TiO_2, Nb_2O_5 and V_2O_5, [17-21] (colorless-brown PC), silver halides [22], alkali halides [23], alkaline earth halides [24], complex minerals [4] (colorless-purplish PC) and titanates [25] (colorless-brown PC). However, most of them are in form of thin films or single crystals, and PC phenomena in some materials are usually caused by unavoidable impurities of transition metal ions. They usually exhibit a high-cost preparation, poor PC reversibility, narrow response in the spectrum and slow response time [26]. As a matter of fact, in addition to these weaknesses, photochromic materials as single crystals are less useful than in powder form for many applications. Photochromic materials in powder form can lend themselves particularly well to large area displays and their surface color is ideally suited to reflective readout in ambient light [27]. So, it is of great interest to synthesize PC materials in powder form. Very recently, some inorganic PC powder materials have been reported, including $BaMgSiO_4:Eu^{2+}$ (colorless-pink PC), $Sr_2SnO_4:Eu^{3+}$ (colorless-purple PC), $CaAl_2O_4:Eu^{2+}$, Nd^{3+} (colorless-purple PC), $Ba_5(PO_4)_3Cl:Eu^{2+}$ (colorless-amethyst PC), $Zn_2GeO_4:Eu^{2+}$ (colorless-light gray PC), $ZnGa_2O_4:Bi^{3+}$ (colorless-gray PC) and $LiGa_5O_8:Cr^{3+}$ (cyanish-reddish PC) [28-34]. Notably, the

School of Physics and Optoelectronic Engineering, Guangdong University of Technology, WaiHuan Xi Road, No.100, Guangzhou 510006, China.Email : huyh@gdut.edu.cn; Fax: +86 20 39322265; Tel: +86 20 39322262;
† Footnotes relating to the title and/or authors should appear here.
Electronic Supplementary Information (ESI) available: [details of any supplementary information available should be included here]. See DOI: 10.1039/x0xx00000x

photochromism of oxide semiconductors involves photo-generated electrons/holes migrating in the semiconductors and producing color centers. The color centers absorb visible lights within a certain wavelength range, leading to the color change. As this respect into consideration, the choosing of dopants which can cause color centers in a suitable host is a prerequisite for photochromism. Among the PC powder materials mentioned above, europium ion is the mostly used as dopant into inorganic compounds, exhibiting excellent PC properties, i.e. high physical and chemical stability, excellent PC reversibility and good thermal stability.

In other aspect, the insights into the PC mechanism are useful for determining which materials may possess good PC properties, thereby giving a guideline to synthesize excellent PC powder materials. Several models, such as F-center model, small polaron model and electron/hole traps model, have been put forward to explain the PC mechanism [29, 35]. Unfortunately, the details are still unknown and the synthesis of PC powder materials is still by trial and error. Hence, the synthesis and deeper characterization of novel PC powder materials are not only the requirement of practical use but also the developing and perfection of PC mechanism.

As a proof of concept, a set of Eu^{2+}-doped belovite-type halo-phosphates powders with the formula $Sr_{3-x}YNa(PO_4)_3F:xEu^{2+}$ were prepared successfully for the first time by a conventional high temperature solid state reaction method. All as-obtained samples show reversible colorless-cyan PC property when alternately irradiated by short wavelength light (200-320 nm) and longer wavelength light (320-800 nm). The light induced cyan color in inorganic PC powders has never been reported to the best of our knowledge. The reflectance dependence of the powder by different wavelengths irradiation on time in coloration and bleaching processes were studied. The colored surface also can be bleached quickly under thermal treatment. It shows high fatigue resistance in PC and heat treatment bleaching process. Furthermore, based on thermoluminescence (TL) measurements, two kinds of traps generated in host lattice are responsible for the occurrence of PC in $Sr_3YNa(PO_4)_3F:Eu^{2+}$. The dynamic motion of electrons between two different traps in coloring and bleaching processes was studied in detail. At last, a model was constructed to deeply elaborate the PC mechanism.

2. Experimental

2.1 Materials synthesis

The powder samples with nominal formula $Sr_{3-x}YNa(PO_4)_3F:xEu^{2+}$ (SYNPF:xEu^{2+}, x=0.002, 0.005, 0.007, 0.01, 0.02, 0.03, 0.04 and 0.05) were synthesized via a traditional high temperature solid-state reaction method. The raw materials are analytical $SrCO_3$, SrF_2, Y_2O_3, Na_2CO_3, $(NH_4)_2HPO_4$ and Eu_2O_3 (99.99%). All starting reactants were weighed according to stoichiometric ratio except that 20% excess of SrF_2 was used for the loss of fluorine. After mixed and ground thoroughly, the mixtures were first heated at 600 °C for 2 h in ambient atmosphere. After cooling down naturally to room temperature (RT), the powders were ground again and then calcined at 1100 °C for 3 h under a reductive atmosphere (85% N_2+15% H_2). A blank sample [non-doped $Sr_3YNa(PO_4)_3F$] and Eu^{3+}-doped $Sr_3YNa(PO_4)_3F$ were also prepared with the same method but in ambient atmosphere. Finally, all as-obtained samples were furnace-cooled to room temperature and reground to fine powders for the following measurements.

2.2. Measurements and characterization

The phase structure of all as prepared sample were characterized by powder X-ray diffraction (XRD) using a XD-2 powder diffractometer operating at 36 KV and 20 mA with Cu Kα irradiation (λ=1.5406 Å) at continuous scanning step of 0.02° in the 2θ range from 10° to 70°. The chemical compositions of SYNF:$0.005Eu^{2+}$ were analysized by X-Ray Fluorescence (xrf-1800, Shimadzu). The surface morphology of the prepared powder was examined with a field emission scanning electron microscope (SEM) equipped with an energy dispersive spectrometer (EDS) (Nova NanoSEM 450, Netherlands). Photoluminescence excitation (PLE) and photoluminescence (PL) spectra were measured by a FLS-980 fluorescence spectrophotometer with Xe 900 (450 W xenon arc lamp) as the light source. Diffuse reflectance spectra of samples were collected by an UV-2450 spectrophotometer (Shimadzu UV-2450, Japan) using $BaSO_4$ as a reference. High temperature diffuse reflectance spectra were measured with the assistance of a homemade heating instrument. The thermoluminescence (TL) curves were recorded by a FJ-427A1 meter (Beijing Nuclear Instrument Factory) with a heating rate of 1 °C/s. Electron paramagnetic resonance (EPR) spectra were obtained on an A200-9.5/12 electron paramagnetic resonance spectrometer at a frequency 9.18 GHz at room temperature (air atmosphere) and low temperature (77 K) in vacuum.

3. Results and discussion

3.1 Phase identification and crystal structure

The XRD patterns of three representative as-obtained samples SYNPF:xEu^{2+} (x=0, 0.01 and 0.04) and the standard XRD data of $Sr_3(La,Ce)Na(PO_4)_3(F,OH)$ are shown in Fig. 1(a) for comparison. All the diffraction peaks can be almost well indexed to the standard data of JCPDS 50-1595, which indicates that the as-prepared materials are isostructural with $Sr_3(La,Ce)Na(PO_4)_3(F,OH)$ (hexagonal crystal system with the space group $P\bar{3}$ (147)) reported in the database of the Joint Committee on Powder Diffraction Standards.

No impurity or any significant change can be detected evidently with the incorporation of Eu^{2+} into SYNPF host, inferring phase

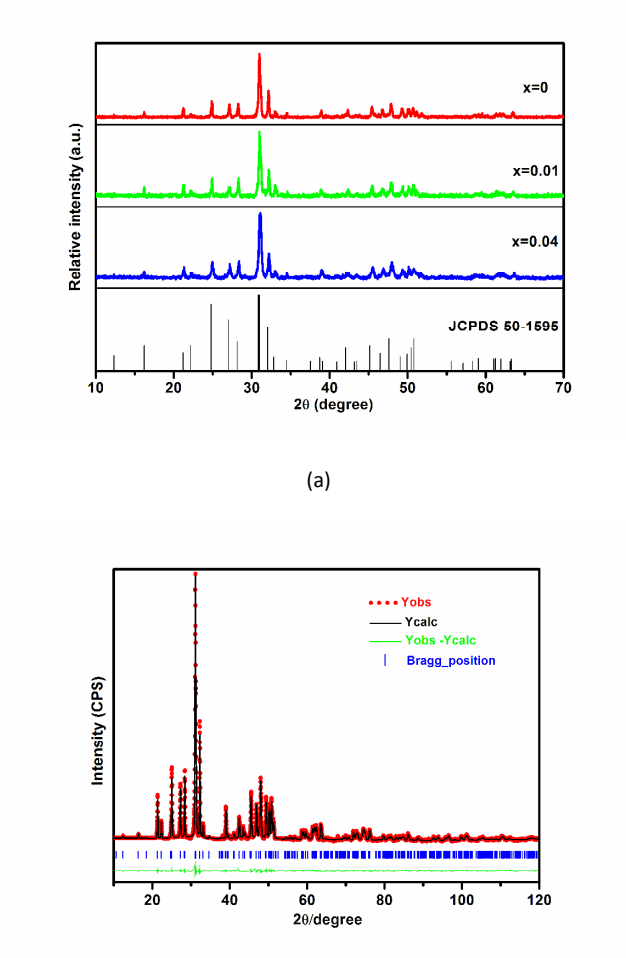

Fig. 1 (a)XRD patterns of samples SYNPF:xEu^{2+} (x=0, 0.01 and 0.04) and the comparison with JCPDS standard data (no. 50-1595). (b)Experimental (red dots) and calculated (black solid line) powder XRD patterns of the SYNPF sample. The green solid lines mean the difference between experimental and calculated data, and the blue sticks mark the Bragg reflection positions.

purity of the all as-obtained products. Taking the closer ionic radii and valence state between Sr^{2+} and Eu^{2+} ions into consideration ($r_{Sr^{2+},CN=6}$ =1.18 Å, $r_{Eu^{2+},CN=6}$ =1.17 Å, $r_{Gd^{3+},CN=6}$ =0.94 Å and $r_{Na^{+},CN=6}$ =1.02 Å) [36], Eu^{2+} is assumed to preferentially substitute for the Sr^{2+} sites. Rietveld structure refinement of sample SYNPF was performed using the general structure analysis system (GSAS) program [37] to obtain the detailed crystal information. Fig. 1(b) gives the refinement pattern of SYNPF. The final structural parameters are listed in Table S1†. The reliability factors R_{wp}=3.97%, R_p=2.74% and χ^2=2.98 indicate that atom positions and fraction factors of the refined sample SYNPF well satisfy the reflection conditions. SYNPF is crystallized in a $P\bar{3}$ space group with lattice parameters of a=b=9.627241 Å, c=7.133053 Å and V=572.545 $Å^3$.

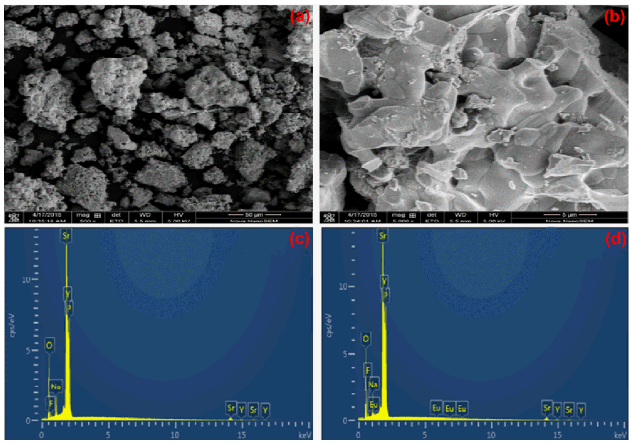

Fig. 2 SEM images of the SYNPF host (a) and SYNPF:0.005Eu^{2+} (b); EDS spectra of the SYNPF host (c) and SYNPF:0.005Eu^{2+} (d).

Fig. 2(a) and (b) present the SEM images of the non- and Eu^{2+}-doped SYNPF host, respectively. It can be seen that the obtained powders consist of particles with size around several microns which usually occur in high temperature solid state reaction. The morphology of the as-prepared grains presents a smooth surface. The EDS results in Fig. 2(c) and (d) reveal the presence of Sr, Y, Na, P, O and F in the undoped SYNPF and Sr, Y, Na, P, O, F and Eu in Eu^{2+}-doped SYNPF host, respectively. As shown in Fig. 2(c), the atoms ratio of undoped SYNPF was determined to be about Sr:Y:Na:P:O:F=3.03:1:1.05:3.08:12.60:0.85. The experimental result is almost in agreement with the theoretical value of SYNPF, indicating the formation of the molecular formula. Fig. 2(d) infers the successful incorporation of Eu^{2+} into SYNPF host lattice. The chemical compositions of the SYNPF:0.005Eu^{2+} are also analyzed by XRF, as listed in Table S2†. According the weight ratio, the calculated molar ratio is close to n(Sr):n(Y):n(P):n(Na):n(Eu):n(F)=3:1:3:1:0.005:1.

3.2 Photoluminescence and photochromism properties of SYNPF:Eu^{2+}

Fig. 3(a) shows the excitation and emission spectra of the obtained powder SYNPF:0.005Eu^{2+}. The excitation spectrum monitored at 456 nm exhibits a broad band ranging from 210 to 430 nm, which can be attributed to the electron transitions from the ground state $^8S_{7/2}$ ($4f^7$) to the crystal-field split components of $4f^6$5d states. Upon excitation by 292 nm, the emission spectrum shows an broad band ranging from 400 to 550 nm with the maximum at 456 nm due to the $4f^6$5d-$4f^7$ transition of the Eu^{2+} ions.

Fig. 3(b) shows the diffuse reflection spectra of SYNPF:0.005Eu^{2+} after irradiated by different wavelength light for 3 min. The change

of body color due to UV irradiation can be qualitatively reflected by measuring the diffuse reflectance on the samples. The powder SYNPF:0.005Eu^{2+} absorbs light in a broad wavelength region (350-800 nm) after UV-light irradiation.

The absorptions around 450 and 596 nm increase significantly. Therefore, the surface color of SYNPF:0.005Eu^{2+} quickly turns cyan by UV light irradiation (200-320 nm) and also can be substantially bleached after visible light irradiation in room light condition as presented in Fig. 3(d). The value of (1-R)% is defined as the measurement of color change degree (The higher value is, the surface color changes greater). As shown in Fig. 3(c), the values of (1-R)% at 596 nm are plotted as a function of different irradiation wavelengths. It is notable that the effective wavelength induced photochromic phenomenon only ranges from 200 to 320 nm, which gives an evident difference when compared with excitation spectrum and indicates that only UV light with higher energy can induce the PC phenomenon. The result infers that the reflectance of SYNPF: Eu^{2+} strongly depends on the wavelength of irradiation lights. Essentially, the reflectance spectrum is decided by the transition probability of electrons, because that the transition probability largely depends on the wavelength of irradiation light [38]. Consequently, it is supposed that PC process could be ascribed to the electron storage in electron traps in this material. Under UV excitation, the electrons can be captured by electron traps resulting in PC only when they are excited into higher 4f^{6}5d^1 states of Eu^{2+} ions. If hole traps are supposed to be dominated in the generation of PC, upon UV irradiation, the holes can be left in the ground state

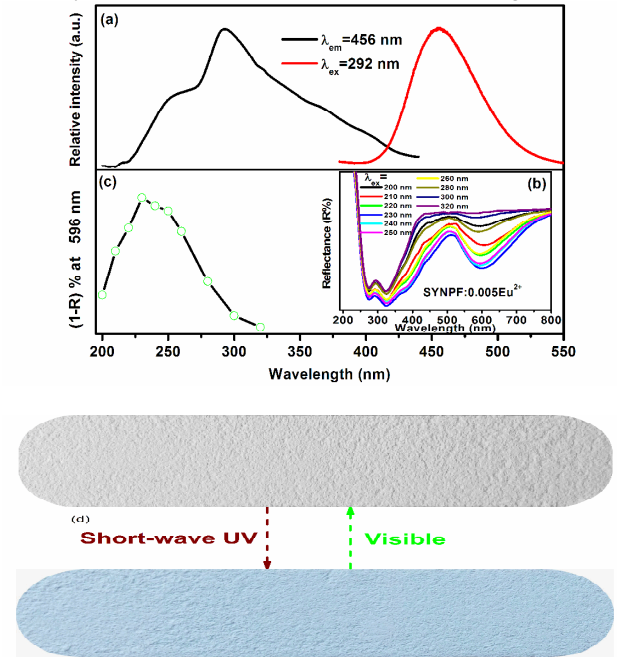

Fig. 3 (a) Excitation (λ_{em}=456 nm) and emission (λ_{ex}=292 nm) spectra of SYNPF:0.005Eu^{2+}; (b) Diffuse reflectance spectra of SYNPF:0.005Eu^{2+} after irradiated by different wavelength light (200-320 nm) for 5 min; (c) Irradiation wavelength dependence of the reflectivity intensity at 596 nm for SYNPF:0.005Eu^{2+}; (d) Corresponding paragraphs of the photochromic performance.

of Eu^{2+} ions. Afterwards, holes can enter into valence band and then captured by hole traps. However, this process should not be affected by the case that electrons are either excited into higher or lower excited states of Eu^{2+} ions, which indicates the identical shape between excitation spectrum in Fig. 3(a) and that in Fig. 3(c).

Fig. 4 gives the response of sample SYNPF:0.005Eu^{2+} to light irradiation of 230 nm. The value of (1-R)% at 596 nm increases drastically with the increasing of irradiation time, indicating the

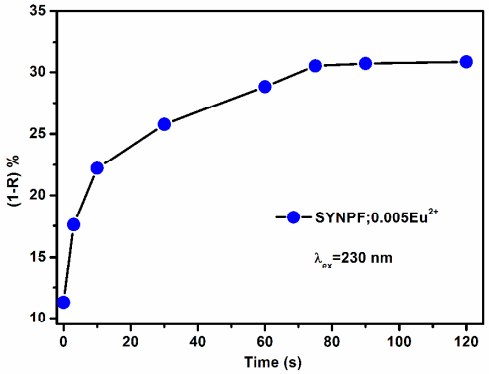

Fig. 4 The dependence of (1-R) % values at 596 nm on irradiation time by 230 nm for SYNPF:0.005Eu^{2+}.

coloring processes. It reaches a steady state at about 75 s and hardly changes any more. The result infers that the reflectance of SYNPF: Eu^{2+} is also influenced by light irradiation time. When the electron traps are filled with electrons and saturated at 75 s under UV irradiation light of 230 nm, no more electrons can be captured by electron traps. As a reversible photochromic material, the decoloration properties of SYNPF:Eu^{2+} should be studied. After irradiated by 230 nm for 3 min, the reflectance dependence of sample SYNPF:0.005Eu^{2+} on the wavelength of irradiation light (300-800 nm) and irradiation time (1s-180s) is exhibited in Fig. 5. The decoloration process is not only influenced by the wavelength of irradiation light but also irradiation time, which is the same as that in coloration process [see in Fig. 3(c) and Fig. (4)]. It can be bleached by irradiation light (320-800 nm). Therefore, the bleaching process of colored sample can be observed under sunlight for several minutes. Though the bleaching can be induced by light irradiation in a broad wavelength range, there is a selective wavelength priority. The most effective bleaching wavelength range is determined to be 320-475 nm. The decoration process of colored SYNPF:Eu^{2+} occurs quickly when exposed into light (320-475 nm). It can be completely bleached by light irradiation (320-475 nm) for about 10 s. The light irradiation between 550 and 700 nm is the secondarily effective wavelength range for the bleaching of colored SYNPF:Eu^{2+}. In this case, the colored sample can be substantially bleached when the

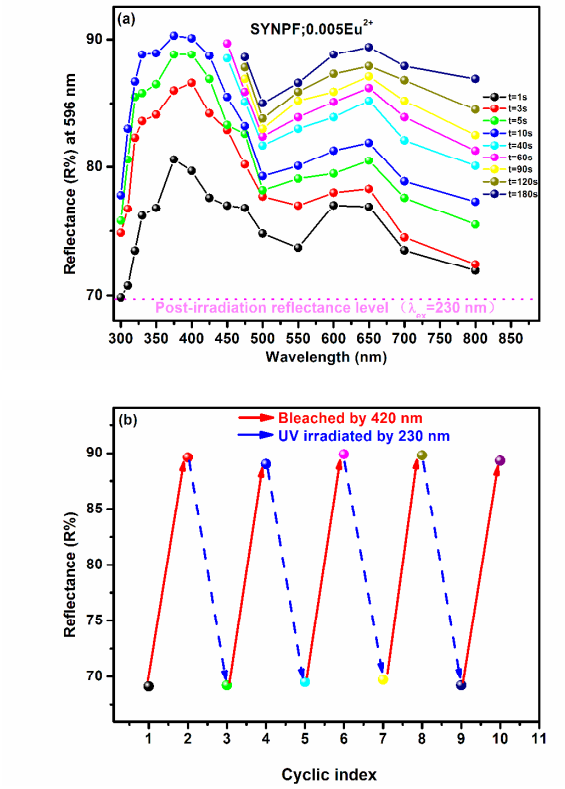

Fig. 5 (a) Reflectivity intensity changes at 596 nm for SYNPF:0.005Eu^{2+} after irradiated by different wavelength light (300-800 nm) for different dwell times (SYNPF:0.005Eu^{2+} is completely colored before the measurements); (b) Reflectance changes of SYNPF:0.005Eu^{2+} at 596 nm induced by alternating 230 and 420 nm light irradiation.

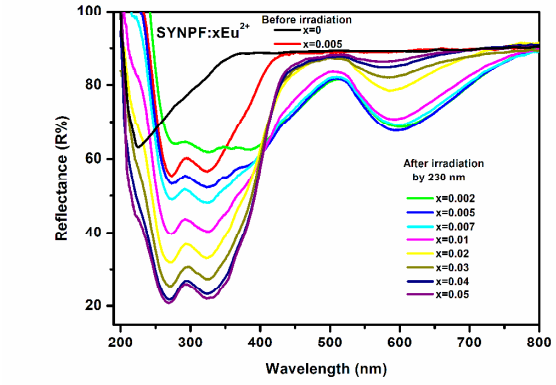

Fig. 6 Reflectance spectra of samples SYNPF:xEu^{2+}(x=0 and 0.005) before irradiation and SYNPF:xEu^{2+}(x=0.002-0.05) after irradiation by 230 nm for 5 min.

irradiation time reaches about 180 s. Fatigue resistance is one of the most important requirements for a photochromic material [7]. Fig. 5(b) shows the coloring-bleaching and the color density change process of SYNPF:Eu^{2+} when irradiated alternatively by 230 nm and 420 nm. It shows a high reversibility in the coloration-bleaching processes. The results indicate that the recording and erasing of information in SYNPF:Eu^{2+} can be well repeated, suggesting that SYNPF:Eu^{2+} may be potentially used as photoswitches and high density optical memories.

Fig. 6 shows the reflectance dependence on Eu^{2+} doping concentration. In addition, Non-doped SYNPF is shown as a blank reference. The reflectivity of SYNPF host starts to decrease gradually from 350 nm which is caused by the host absorption. When Eu^{2+} is doped into SYNPF host, it shows a notable drop before 440 nm, which is caused by the absorption of Eu^{2+} ions. After irradiation by 230 nm, the reflectivity of SYNPF:Eu^{2+} between 400 and 750 nm especially at 450 and 596 nm exhibits a significant decrease. The reflectivity at 450 and 596 nm strongly depend on the Eu^{2+} doping concentration. It decreases at first, reaching the minimum at x=0.005, and then it turns to be increased continuously, which infers that the best photochromic properties can be obtained when 0.5% mol Eu^{2+} is incorporated into SYNPF host. The trap density which is related to Eu^{2+} doing concentration plays a critical role.

3.3 Cyan surface color fading of SYNPF:Eu in dark at room temperature

Generally, the lifetime of color in light induced photochromism in inorganic materials can persist from a few seconds to a few days [1, 39]. In SYNPF:Eu, UV light induced coloration phenomenon is long lived at room temperature and can last for more than one month (the coloration still can be observed evidently one month after the UV light induced sample is stored in the dark). So it is of great importance to investigate the change of reflectance spectra with time. Fig. 7(a) shows the time resolved reflectance spectra from 0 to 384 h after the removal of UV-irradiation (230 nm). The shapes are similar but the intensity of reflectance increases with time, indicating the slow liberation of captured electrons from traps. The function of reflectivity at 596 nm versus waiting time is plotted in Fig. 7(b). It is seen that the UV-induced color maintains about half of

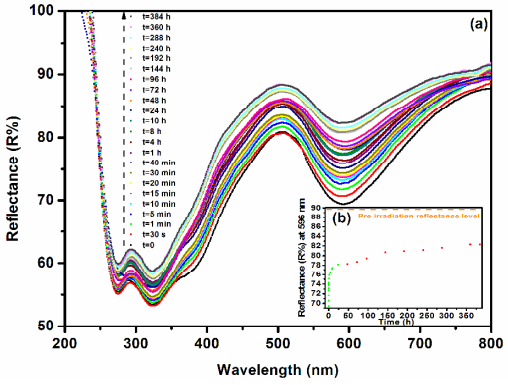

Fig. 7 (a) Reflectance spectra of SYNPF:0.005Eu^{2+} at different delay time in dark after irradiated by 230 nm for 5 min; (b) Reflectivity intensity (at 596 nm) dependence on different delay times (0-384 h), green and red dots represent fast and slow decoloration processes, respectively.

the initial coloration level even when the delay time increases to 384 h. In the first 24 h, the reflectivity increases very fast. Then, it becomes slowly with longer delay time. Two different bleaching

processes are distinguished, inferring the existence of two different types of traps in host lattice with shallow and deep depths which control the fast and slow bleaching processes, respectively.

3.4 Thermoluminescence properties

In order to further understand the nature of electron traps and photochromic centers in SYNPF:Eu, thermoluminescence (TL) measurements on SYNPF:Eu powders were conducted. As shown in Fig. S1(a)†, TL curves of samples SYNPF:xEu^{2+} (x=0.002, 0.005, 0.007, 0.01, 0.02, 0.03, 0.04 and 0.05) were collected after irradiated by 254 nm for 3 min with 5 min delay time. They show the similar shape, but the TL intensity is strongly dependent on Eu^{2+} doping concentration. The integral area of the TL curve represents the fact that traps capture the gross amount of charge carriers. TL integral intensity of all as-obtained Eu^{2+}-doped samples show the similar change trend as that in reflectance spectra (Fig. 6), indicating that the photochromic property is closely related to the traps and Eu^{2+} centers in host lattice. When the amount of Eu^{2+} is 0.5 mol % in SYNPF, the maximum TL intensity could be obtained. The broad TL spectrum covers from 35 to 350 °C and can be deconvoluted into two distinguished peaks 1 and 2 centered around 107 and 212 °C, respectively [Fig. S1(b)†]. In Eu^{2+}-doped SYNPF, the traps are mainly caused by intrinsic defects oxygen vacancies which can serve as electron traps in host lattice. The incorporation of Eu into SYNPF host lattice substituted for Sr sites, which promotes the generation of Sr vacancies. Low density Sr vacancies in SYNPF can be beneficial to the increase of TL intensity as they can lower the formation energy of oxygen vacancies. On the contrary, high density Sr vacancies should be detrimental to the generation of electron traps since that they are highly likely to be located near Eu^{2+} and transform the Eu^{2+} to higher valence states [40]. According to the equation $E=T_m/500$ (T_m is the temperature at TL peak) provided by Chen [41]. The trap depths (E) of peaks 1 and 2 are estimated to be about 0.76 and 0.97 eV, respectively. Generally, the temperature of TL peak situated between 50–120 °C is suitable for the charge carriers escaping from traps at room temperature. Charge carriers are not easy to be released by deeper traps (at higher temperature) [42, 43]. Therefore, it is speculated that TL peaks 1 and 2 are responsible for the fast and slow decoloration processes, respectively. Fig. 8(a) shows the TL curves on SYNPF:0.005Eu undergoing different delay times from 5 min to 384 h after the stoppage of UV-irradiation (230 nm) for 3 min. A majority of the shallow-trap (at peak 1) disappears gradually and the deep-trap (at peak 2) still exists when the delay time increases to 384 h, which demonstrates the speculation above and indicates that electrons captured by deep traps may transfer to shallow traps. The photo-stimulation method is frequently used to study the photochromic centers in storage materials [44]. As shown in Fig. 8(b), the TL curve of the 288 h-delayed SYNPF:0.005Eu powder after being exposed to 420 nm for 5 s was measured along with the counterpart without photostimulation. Compared with the TL curves of 288 h-delayed sample with and without 420 nm light stimulation, it is notable that the peak intensity of deep trap decreases while the shallow one appears. It verifies that some electrons in the deep traps can be photo-released, transferred and then captured by the emptied shallow traps. This phenomenon also have been observed elsewhere [45]. The external stimulation accelerates the electron release from traps, leading to the faster decoloration at room temperature. To explore the electrons motion between traps with different depth, TL glow curves of SYNPF:0.005Eu were also recorded after irradiated by 254 nm for different times (t=5, 10, 30, 60 and 90 s) with delay time of 5 min. As shown in Fig. S2(a)†, the TL integral intensity increases as the irradiation time is prolonged. The TL intensity rations of (Peak 2)/(Peak 1) are listed in Fig. S2(b)†. The value increases at first, reaching maximum at t=30 s and then keeps almost a constant. It indicates that the excited electrons preferentially fill the shallow traps, accompanied with electron transfer from shallow traps to deep traps and finally reaching a dynamic equilibrium. Thus, it can be concluded that traps with different depths are not independent: electron can transfer from shallow traps to deep traps in coloring process and then move backwards in photon induced bleaching process.

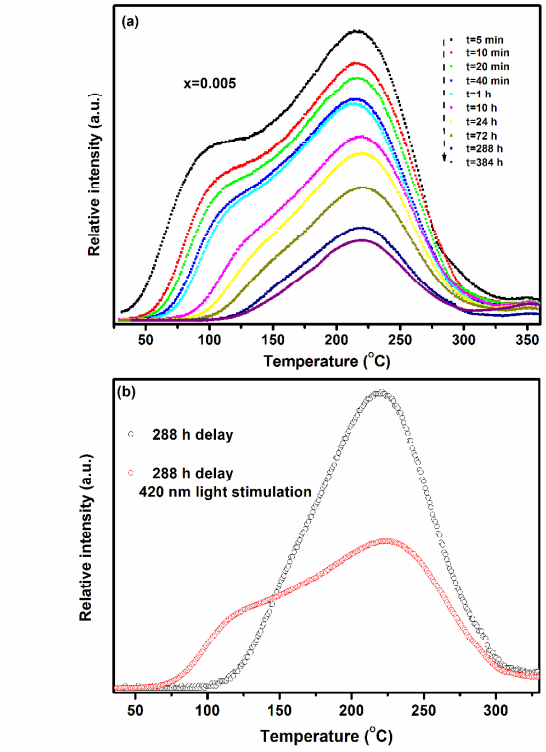

Fig. 8 (a) TL glow curves of SYNPF:0.005Eu^{2+} after irradiated by 254 nm for 5 min with different delay times (5 min-384 h); (b) TL glow curves of SYNPF:0.005Eu^{2+} after irradiated by 254 nm for 5 min at delay time t=288 h without (black dots) and with (red dots) 420 nm light stimulation.

3.5 Cyan surface color fading by thermal treatment

The UV irradiation induced coloration not only can be quickly bleached by external stimulations, but also by thermal treatment. We investigated the influence of temperature on the reflectance of the SYNPF:0.005Eu. Fig. 9(a) gives the reflectance dependence on the heating temperature. The reflectance especially the drops centered at 450 and 596 nm increases drastically with the rising of heating temperature. The colored SYNPF:0.005Eu is almost substantially bleached after thermal treatment of 240 °C. Fig. 9(b) shows the dependence of the reflectance at 593 nm on the temperature of heat treatment. It is clearly seen that the reflectance increase under thermal treatment experiences two processes. The linear fitting results indicate a slow increasing process below 120 °C and a fast increasing process above 120 °C.

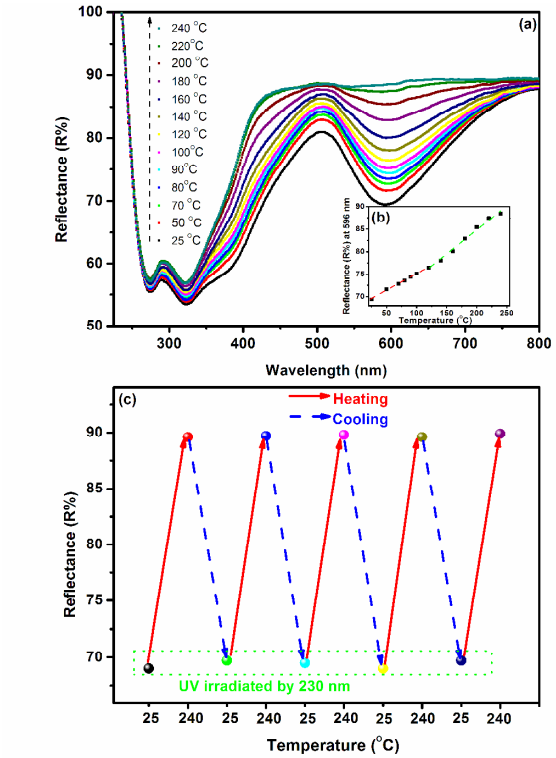

Fig. 9 (a) Reflectance spectra of SYNPF:0.005Eu^{2+} after heating treatment at different temperatures (25-240 °C) for 3 min; (b) Dependence of reflectivity at 596 nm on heating temperature: red and blue lines indicates fast and slow bleaching processes, respectively; (c) Reflectivity changes at 596 nm by alternating 230 nm irradiation (after cooling down to room temperature) and heating treatment at 240 °C for 3 min.

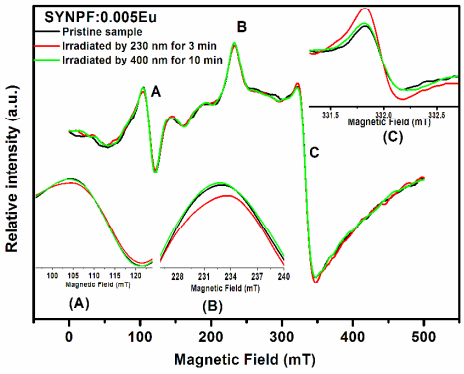

Fig. 10 EPR spectra of SYNPF:0.005Eu^{2+} with and without irradiation by 230 nm for 3 min as well as the colored sample irradiated by 400 nm for 10 min below room temperature (77 K) in vacuum.

The slow increasing process is caused by the elimination of electrons from shallow traps (TL peak 1). When the heating temperature is higher, the elimination of electrons from both shallow (TL peak 1) and deep traps (TL peak 2) gives rise to the fast increasing process. Fig. 9(c) shows reversibility in the coloration-decoloration processes with alternative heating and irradiation by 230 nm. The intensity of the reflectance at 593 nm is repeatedly recovered to the initial level by 240 °C treatment when the random errors during measurements are considered, indicating high fatigue resistance of photochromic properties in heat treatment. There is almost no severe thermal degradation for the PC performance after several cycle experiments, implying good PC thermostability of SYNPF:Eu.

3.6 EPR analysis

The EPR spectra of the sample SYNPF:0.005Eu without and with irradiation by 230 nm for 3 min as well as the colored sample irradiated by 400 nm for 10 min were recorded below room temperature (77 K) in vacuum, as illustrated in Fig. 10. In general, the EPR of Eu^{2+} ion in an isotropic crystal field exhibits seven sets of fine structures resulting from the transitions between the different m_j levels (7/2, 5/2, 3/2, 1/2, -1/2, -3/2, -5/2 and -7/2, $\Delta m_j=\pm1$) [46]. The obtained EPR signals are associated to overlap of Eu^{2+} and the paramagnetic singly ionized oxygen vacancy ($V_O^{\cdot}$) [47,48,49]. The zoom EPR spectra of two sharp EPR signals A and B are shown in Fig. 10(A) and (B), respectively. It is obvious that in both cases the intensity of EPR signal shrinks after irradiated by 230 nm and then almost regains the initial level, inferring that Eu^{2+} ions are converted into Eu^{3+} under 230 nm irradiation and then the trapped electrons return to Eu^{3+} through CB upon 400 nm irradiation. However, the change of signal C shows an opposite case. As exhibited in Fig. 10(C), it can be observed from the zoom EPR spectra that the intensity of EPR signal increases after irradiated by 230 nm and then almost decreases to the initial level. This is attributed to the overlap of EPR signals between Eu^{2+} and $V_O^{\cdot}$. Under excitation by 230 nm, numerous $V_O^{\cdot}$ are generated, which compensates for the EPR signal decrease caused by $Eu^{2+}\rightarrow Eu^{3+}$. In addition, the EPR spectra of the sample SYNPF:0.005Eu without and with irradiation by 230 nm for 3 min were also collected at room temperature (25 °C) in air atmosphere, as exhibited in Fig. S5†. It is difficult to identify all fine structure lines when Eu^{2+} ions locate in the host lattice with lower symmetry, particularly in powder materials [50]. In view of this, the broad signal with unresolved hyperfine line centered at 3514 G corresponding to the g value of 2.001 is attributed to 1/2↔-1/2 magnetic dipole transition [51, 52, 53] of Eu^{2+} in SYNPF host. It is notable that the EPR signal intensity of the sample SYNPF:Eu^{2+} decreases after irradiated by 230 nm. The intensity of EPR signal of Eu^{2+} should correlate with the concentration of Eu^{2+} ions in SYNPF host. The weakening of EPR signal infers a decreasing amount of Eu^{2+}, indicating that Eu^{2+} ions are converted into Eu^{3+} with the irradiation.

3.7 Photochromism mechanism for SYNPF:Eu^{2+}

According to the results and discussions above, a PC mechanism is proposed on the basis of a model constructed by us. Firstly, the bandgap (~5.66 eV) can be roughly derived from the reflectance spectrum of undoped SYNPF (Fig. 6). The ground level and lowest 5d state of Eu^{2+} should be determined. Based on P. Dorenbos [54, 55], the ground state position of Eu^{2+} can be roughly estimated on the basis of CT energy (charge transfer of O^{2-}-Eu^{3+}). Therefore, it seems that the ground level of Eu^{2+} locating at ca. 4.92 eV above the top of the

VB (valence band) of SYNPF can be derived from Fig. S3†. However, it is not the case as it loos. In fact, there is a large deviation between them and the obtained CT energy is much higher than the ground state of Eu^{2+}. This is largely due to two factors: one is the influence by defects; another is that Eu^{3+} and Eu^{2+} go into different sites (Y and Sr sites, respectively) with different coordination numbers or crystal fields in crystal lattice. As shown in Fig. S4 (a) and (b)†, the luminescence quenching activation energy 0.342 eV which indicates the energy difference between the lowest 5d level of Eu^{2+} and the CB (conduction band) bottom of SYNPF host is obtained. The emission energy (2.72 eV) can be obtained from the elementary photoluminescence studies. Thereby, a model is constructed and illustrated in Fig. 11. Upon UV (λ_{ex}<400 nm) and blue radiation (400 nm<λ_{ex}<430 nm), the 4f electrons can be excited from ground state into higher empty 5d (H-5d) (process ①) and lower 5d (L-5d) (process ②) excited states of Eu^{2+} ions [56], respectively, leaving 4f levels unoccupied. Blue emission originating

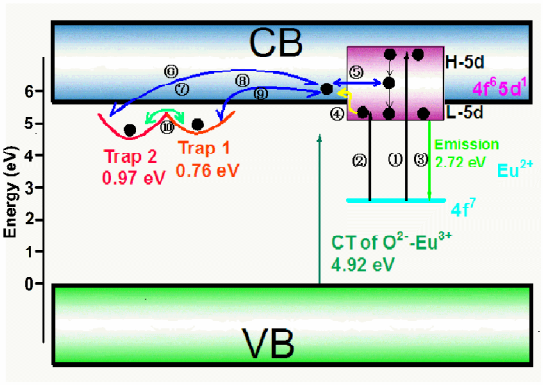

Fig. 11 Schematic diagram for illustration of PC mechanism.

from Eu^{2+} can be observed when the majority of electrons in 5d levels move back into the 4f levels (process ③). Besides, the minority of electrons may escape from L-5d states into CB with the aid of thermal energy (process ④) in spite of small possibility at room temperature. The residual electrons in higher H-5d states can easily be transferred into the low-CB, becoming free electron carriers, and then move to elsewhere in the crystal (process ⑤). They may be captured by empty defect levels (traps) exist just below the CB with different depts. In this processes, they are easily and mainly trapped by shallow traps (trap 1) (process ⑧) accompanying electron transfer to deep traps (trap 2) (process ⑩) as well as very few of them may be trapped by trap 2 directly (process ⑥). The trapped electrons form F-like color centers. Consequently, the surface color of SYNPF:Eu powder changes to cyan. When the colored powder is placed in dark room, electrons in trap 1 will gradually escape and move back into CB (process ⑨). Then, they will move to the Eu^{2+} 5d states (process ⑤) and finally jump back to 4f levels, which leads to fast bleaching process at first [see in Fig. 7(b)]. However, electrons in trap 2 can not be easily released directly into CB at room temperature in dark. They can further move to trap 1 at a very low rate which results in the subsequent slow bleaching process [see in Fig. 7(b)]. In contrast, the bleaching process is largely accelerated when external intervention such as irradiation by light or heating is used. It can facilitate the electrons release from trap 1 to CB and electrons transfer from trap 2 to trap 1 or CB directly when the colored SYNPF:Eu powder is irradiated with light (320-800 nm). Though the detail is not clear, we preliminarily assume that the wavelength selective dependence in bleaching property is related to the traps distribution in the host. When shorter wavelength irradiation (320-475 nm) is applied, electrons in trap 2 can be directly impelled to trap 1 or released into CB(process ⑦), resulting in fast bleaching process. When longer wavelength irradiation (550-700 nm) is used, it may just facilitate the escaping of electrons from trap 1 into CB and moving of electrons from trap 2 to trap 1 [see in Fig. 8(b)], leading to a slower bleaching phenomenon. On heating, the trapped electrons directly transfer from traps to CB, which is also an effective way to realize the decoloration.

4. Conclusions

In summary, a series of Eu^{2+} doped $Sr_3YNa(PO_4)_3F$ powders were successfully synthesized by a conventional high temperature solid state reaction method. Interestingly, they show reversible colorless-cyan photochromism properties. The surface color of SYNPF:Eu^{2+} turns cyan upon light irradiation (200-320 nm) and quickly changes colorless upon light irradiation between 320 and 800 nm or by thermal treatment. The optimal doing concentration of Eu^{2+} for PC properties is experimentally to be 0.5 mol %. The cyan color of the SYNPF:Eu^{2+} powder fades fast at first and then at a very slow rate in dark at room temperature. With the aid of TL measurements, the two different processes are attributed to two traps in host lattice with different depths. The electrons motion between different traps in coloring and bleaching processes were studied in detail. Good photochromic reversibility and thermostability of the obtained photochromic SYNPF:Eu^{2+} powders are confirmed. Accordingly, a model is constructed and the possible mechanism for PC generation in SYNPF:Eu^{2+} is illustrated. Due to the PC properties, SYNPF:Eu^{2+} may be a potential candidate for application as optical storage devices and photoswitches.

Acknowledgements

The authors acknowledge the financial support from the National Natural Science Foundation of China (no. 21471038).

References

1Y. Ohko, T. Tatsuma, T. Fujii, K. Naoi, C. Niwa, Y. Kubota and A. Fujishima, *Nat. Mater.*, 2003, **2**, 29-31.
2S. Nishio and M. Kakihana, *Chem. Mater.*, 2002, **14**, 3730-3733.
3J. Guo, D. Jia, L. Liu, H. Yuan, M. Guo, D. Wu and F. Li, *J. Mater. Chem.*, 2011, **21**, 12202-12205.
4J. A. Armstrong and M. T. Weller, *Chem. Commun.*, 2006, **10**, 1094-1096.
5M. M. Russew and S. Hecht, *Adv. Mater.*, 2010, **22**, 3348-3360.
6C. Schomburg, M. Wark, Y. Rohlfing, G. Schulz-Ekloff and D. Wöhrle, *J. Mater. Chem.*, 2001, **11**, 2014-2021.
7M. Irie, *Chem. Rev.*, 2000, **100**, 1685-1716.
8J. Zhang, Q. Zou and H. Tian, *Adv. Mater.*, 2013, **25**, 378-399.
9H. Tian and S. Yang, *Chem. Soc. Rev.*, 2004, **33**, 85-97.
10J. Ren, T. Wagner, J. Orava, M. Frumar and B. Frumarova, *Appl. Phys. Lett.*, 2008, **92**, 011114.
11A. J. Cohen and H. L. Smith, *Science*, 1962, **137**, 981-981.
12G. Poirier, M. Nalin, L. Cescato, Y. Messaddeq and S. J. Ribeiro, *J. Chem. Phys.*, 2006, **125**, 161101.

13J. Yao, K. Hashimoto and A. Fujishima, *Nature*, 1992, **355**, 624-626.
14A. Bianco, S. Perissinotto, M. Garbugli, G. Lanzani and C. Bertarelli, *Laser Photonics Rev.*, 2011, **5**, 711-736.
15P. Zacharias, M. C. Gather, A. Köhnen, N. Rehmann and K. Meerholz, *Angew. Chem. Int. Edit.*, 2009, **48**, 4038-4041.
16J. Ren, X. Xu, W. Shen, G. Chen, S. Baccaro and A. Cemmi, *Sol. Energ. Mat. Sol. C*, 2014, doi:10.1016/j.solmat.2014.11.005.
17K. Bange, *Sol. Energ. Mat. Sol. C*, 1999, **58**, 1-131.
18R. J. Colton, A. M. Guzman and J. W. Rabalais, *Accounts Chem. Res.*, 1978, **11**, 170-176.
19C. B. cyanberg, *Thin Solid Films*, 1994, **251**, 81-93.
20M. Tubbs, *Phys. Status Solidi A*, 1974, **21**, 253-260.
21S. Nishio, M. Kakihana, H. Eba and K. Sakurai, *Jpn. J. Appl. Phys.*, 2003, **42**, 5670-5671.
22R. Araujo, *Contemp. Phys.*, 1980, **21**, 77-84.
23M. Tubbs and D. Wright, *Phys. Status Solidi A*, 1971, **7**, 155-166.
24C. Catlow, *J. Phys. C: Solid State Phys.*, 1979, **12**, 969.
25B. Faughnan, *Phys. Rev. B*, 1971, **4**, 3623.
26T. He and J. Yao, *Prog Mater Sci*, 2006, **51**, 810-879.
27R. Duncan, B. Faughnan and W. Phillips, *Appl. Optics*, 1970, **9**, 2236-2243.
28M. Akiyama, *Appl. Phys. Lett.*, 2010, **97**, 181905.
29S. Kamimura, H. Yamada and C.-N. Xu, *Appl. Phys.Lett.*, 2013, **102**, 031110.
30J. Ueda, T. Shinoda and S. Tanabe, *Opt. Mater. Express*, 2013, **3**, 787-793.
31G. Ju, Y. Hu, L. Chen and X. Wang, *ECS Solid State Lett.*, 2012, **1**, R1-R3.
32Y. Jin, Y. Hu, Y. Fu, Z. Mu and G. Ju, *Mater. Lett.*, 2014, **134**, 187-189.
33Y. Zhuang, J. Ueda and S. Tanabe, *Opt. Mater. Express*, 2012, **2**, 1378-1383.
34F. Liu, W. Yan, Y.-J. Chuang, Z. Zhen, J. Xie and Z. Pan, *Sci. Rep.*, 2013, **3**, 1554 (9 pages).
35M. Rouhani, J. Hobley, G. S. Subramanian, I. Y. Phang, Y. L. Foo and S. Gorelik, *Sol. Energ. Mat. Sol. C*, 2014, **126**, 26-35.
36R. D. Shannon, *Acta Cryst.*, 1976, **32**, 751-767.
37A. C. Larson and R. B. Von Dreele, Los Alamos Natl. Lab.,1994, 1–221.
38S. Shionoya, W. M. Yen and T. Hase, *Phosphor handbook*, CRC press Boca Raton, FL, 1999.
39B. Faughnan and Z. Kiss, *Phys. Rev. Lett.*, 1968, **21**, 1331.
40B. Qu, B. Zhang, L. Wang, R. Zhou and X. C. Zeng, *Chem. Mater.*, 2015, **27**, 2195-2202.
41R. Chen, *J. Appl. Phys.*, 1969, **40**, 570-585.
42K. Van den Eeckhout, A. J. Bos, D. Poelman and P. F. Smet, *Phys. Rev. B*, 2013, **87**, 045126.
43Y. Jin, Y. Hu, H. Duan, L. Chen and X. Wang, *RSC Adv.*, 2014, **4**, 11360-11366.
44 S. Schweizer, *Phys. Status Solidi A*, 2001, **187**, 335-393.
45J. Botterman, K. Van den Eeckhout, I. De Baere, D. Poelman and P. F. Smet, *Acta Mater.*, 2012, **60**, 5494-5500.
46K. Kawano, H. Akahane, R. Nakata and M. Sumita, *J. Alloy. Compd.*, 1995, **221**, 218-226.
47R.-A. Eichel, *Pyhs. Chem. Chem. Phys.*, 2011, **13,** 368-384.
48S. Schweizer, G. Corradi, A. Edgar and J.-M. Spaeth, *J. Phys.-Condens. Mat.,* 2001, **13,** 2331-2338.
49W. W. Ji, M.-H. Lee, L. Y. Hao, X. Xu, S. Agathopoulos and D. W. Zheng, *Inorg. Chem*., 2015, **54,** 1556-1562.
50I. Jaek, G. Hütt, V. Seeman and L. Brodski, *Radiat. Meas.*, 1995, **24**, 557-563.
51V. Singh, V. Natarajan and J.-J. Zhu, *Opt. Mater.*, 2007, **29**, 1447-1451.
52L. Holanda, J. Vargas, C. Rettori, P. Pagliuso, E. Bittar, M. Avila and T. Takabatake, *Physica B*, 2009, **404**, 3300-3303.
53P. Rosa, W. Iwamoto, L. Holanda, R. Ribeiro, P. Pagliuso, C. Rettori and M. Avila, *Phys. Rev. B*, 2013, **87**, 224414.
54P. Dorenbos, *J.Phys.-Condens. Mat.*, 2003, **15**, 8417.
55P. Dorenbos, *J. Lumin.*, 2005, **111**, 89-104.
56J. Qin, H. Zhang, B. Lei, C. Hu, J. Li, Y. Liu, J. Meng, J. Wang, M. Zheng and Y. Xiao, *J. Am. Ceram. Soc.*, 2013, **96**, 3149-3154.

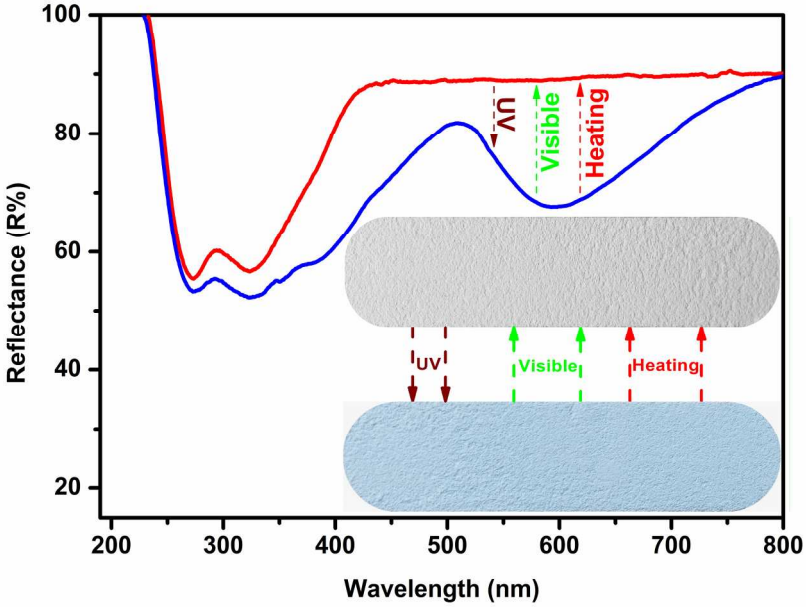

201x141mm (300 x 300 DPI)